

# LONGITUDINAL BEAM MOTION IN THE KEK DIGITAL ACCELERATOR: TRACKING SIMULATION AND EXPERIMENTAL RESULTS

X.Liu<sup>1\*</sup>, T.Adachi<sup>2,3</sup>, S.Harada<sup>3</sup>, T.Iwashita<sup>4</sup>, K.Takayama<sup>1,2,4</sup>, T.Yoshimoto<sup>1</sup>

<sup>1</sup>*Tokyo Institute of Technology, Nagatsuta, Kanagawa, Japan*

<sup>2</sup>*Graduate University for Advanced Studies, Tsukuba, Ibaraki, Japan*

<sup>3</sup>*Tokyo City University, Todoroki, Tokyo, Japan*

<sup>4</sup>*High Energy Accelerator Research Organization (KEK), Tsukuba, Ibaraki, Japan*

## Abstract

Beam commissioning in the KEK Digital Accelerator, which is a small scale induction synchrotron (IS), has been conducted since the middle of 2011. Longitudinal beam motion in the induction synchrotron, utilizing induction cells (IC) for acceleration and confinement, is characterized as barrier bucket acceleration. A tracking code has been developed to understand the longitudinal motion affected by longitudinal space charge forces, considering programmed settings of confinement and acceleration voltage. This code, in which the trigger control scenario is fully implemented, calculates temporal evolution of momentum and phase of macro-particles. Beam commissioning results without acceleration and confinement are compared with simulation results.

## INTRODUCTION

The induction synchrotron concept for accelerating charged particles, was introduced by K.Takayama and his colleagues in 2000[1] and demonstrated using the KEK 12 GeV synchrotron[2] at High Energy Research Organization (KEK). Later this idea had been adapted to the booster ring, which is a rapid cycle synchrotron. For this purpose, necessary modifications and upgrades had been conducted over 3 years. Now it is officially called the KEK Digital Accelerator(KEK-DA). Its details are described in reference [3]. In addition, the ideas and basics behind the KEK-DA are well explained in K.Takayama's text book [4], and the latest status will be presented in this conference.

In this paper, after a short introduction of the KEK-DA system with its layout, the model used to describe the longitudinal motion including longitudinal space charge forces will be discussed. Then the commissioning results and simulation results are shown to be well consistent with each other. Through extensive studies, it turns out that the momentum distribution in the longitudinal phase space is mainly determined by electric fields of the Einzel lens chopper [5] where several  $\mu s$ -long beam is chopped out of a 5 ms-long beam pulse extracted from the ECRIS. The simulations shows that this initial momentum distribution evolves through the low energy beam transport line from the ECRIS to the ring and the beam arrives at the ring with bump profiles both on the beam bunch head and tail. This property in the pulse profile have been observed in the ex-

periment. Further more experiments and simulation works have pursued how the profile evolves in the ring. The simulation will manifest what role space charge forces take in the temporal evolution of the phase space distribution, comparing with experimental data.

## OUTLINE OF KEK-DA

The KEK-DA complex consists of many subsystems just as other accelerator facilities. Fig.1 shows an overview of KEK-DA.

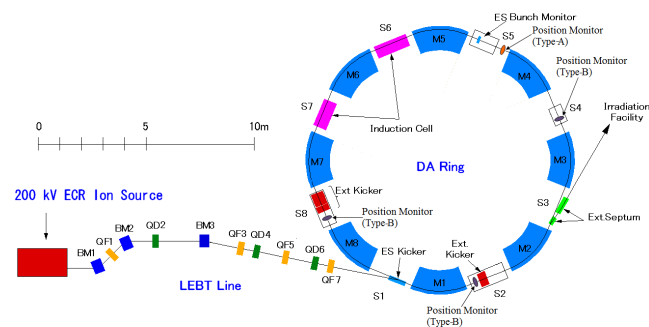


Figure 1: Layout of KEK-DA.

For the present beam commissioning, He<sup>1+</sup> beam is extracted from an Electron Cyclotron Resonance Ion Source(ECRIS)[6] and chopped by the Einzel lens chopper to be several  $\mu s$  beam bunch. The beam bunch is then accelerated to 200 keV by a post-acceleration column installed right after the chopper and guided through Low Energy Transport Line(LEBT). Electrostatic Kicker, installed at one of the drift section (S1 in Fig.1) of the ring, is used to kick the beam bunch on the ring orbit. 8 combined function magnets are installed in the ring to bend the beam and confine it transversely. Induction cells are installed at S6 and S7 section to provide longitudinal confinement and acceleration for the beam bunch. These induction cells are driven by switching power supply [3] powered by DC power supply. Trigger of pulse voltages for acceleration and confinement are fully controlled by the digital control system consisting of the FPGA and DSP[7] A combination of several extraction kickers and septum magnets is used for beam extraction.

\* liuxg@post.kek.jp

## LONGITUDINAL MOTION

### Acceleration Model

The longitudinal equation of motion in the KEK-DA is similar to but different from that of the traditional RF synchrotron. The equations used for a turn-by-turn track in simulations are[4],

$$(\Delta E)_{n+1}^j = (\Delta E)_n^j + Ze[V(\Delta t)_n^j - V_n^s] \quad (1)$$

$$(\Delta t)_{n+1}^j = (\Delta t)_n^j + (T_c)_{n+1}^s \eta_{n+1}^s \left(\frac{\Delta p}{p}\right)_{n+1}^j \quad (2)$$

Eq.1 describes the energy difference  $\Delta E$  for the specific particle with ID “j” to the synchronous particle which is supposed to always stay on the ideal orbit under the ramping magnetic field. In this equation, “n” is the turn number. Z is the charge state (here is positive 1 for He<sup>1+</sup>). e is the unit charge.  $V(\Delta t)$  is the voltage felt by the particle which has a time difference  $\Delta t$  from the synchronous particle.  $V_n^s$  is the required acceleration voltage for the synchronous particle at n-th turn. Eq.2 describes the time difference at n-th turn between a particle with ID j and synchronous particle.  $T_c^s$ ,  $\eta^s$  are revolution time and so-called slippage factor ( $\eta = \frac{1}{\gamma^2} - \frac{1}{\gamma_t^2}$ , where  $\gamma$  is relativistic factor and  $\gamma_t$  is transition gamma), respectively.

As seen in Fig.1, the induction cells with a finite physical size are located at different places. However, the acceleration gap size of each cell is so small that the transit time is negligible. In the model described by the above equation of motion, the acceleration or confinement voltage is assumed to be applied instantly as a  $\delta$ -function like kick. The observation points are chosen to be just in front of the induction cells. As a result, as in the above equations, the energy difference (Eq.1) should be calculated first then this information could be used for calculating new parameters  $T_c$ ,  $\eta$  and  $\frac{\Delta p}{p}$  for Eq.2.

### Longitudinal Space Charge Forces

Injection energy of the KEK-DA is quite low, for example, for He<sup>1+</sup> with the injection energy of 200 keV,  $\beta \approx 0.01$ . Therefore, space charge effects should be significant. The longitudinal space charge forces are evaluated assuming a round beam in a cylindrical chamber model. This model is commonly used, for instance in[8]. The electrical field along the orbit coordinate  $s$  is written by,

$$E_s = \frac{Z_0 g}{4\pi(\beta\gamma)^2 c} \frac{\partial I}{\partial t} + E_W \quad (3)$$

where  $Z_0 = 377\Omega$ , and  $g$  is geometric factor,  $I$  is the beam current,  $c$  is the speed of light.  $E_W$  is the electric field on the chamber wall which is simply ignored in the simulation. In the simulation, an FFT method[8] is used to calculate the electric field instead of directly calculating from Eq.3.

The equation of motion describes the beam motion in a discrete form. This is an exact form without approximation because the induction acceleration devices are localized

at specific positions. Meanwhile the longitudinal space charge forces continuously affect the longitudinal motion of particle. Strictly speaking, the differential equation of motion for the system perturbed with space charge forces must be integrated. Instead of the integration, the differential equation is approximated in the discrete form, where the path length is divided into multiple segments with a small distance and the particle distribution is updated after each segment. Its extreme case corresponds to Eq.1 with a single kick resulting from the space charge forces,  $E_s C_0$ , where the number of segment is just 1; in the other extreme case, the circumference is divided into infinite number of segments. The latter case is unrealistic and we have to choose a finite number of segments.

### Simulation Model

**Justification** Here by justification two things are expected: first, the electric field for a chosen profile should provide the same result as calculated from Eq.3; second, some optimization of the parameters is needed to prevent from producing wrong results. Some common parameters required in Eq.3 and in simulation are assumed as in Table 1. Note that the number of macro-particle and number of bin in Table 1 are parameters used in the FFT method and have been optimized by choosing different combinations of the two so that the electric field in the regions of interest becomes the mathematically calculated value.

Table 1: Parameters Used for Justification

Inj V	g	I
200 keV	6.4161	90 $\mu$ A
beta	N of macro-particle	N of bin
0.0103197	10000	500

Here a trapezoidal profile with 80 ns rise and fall time for beam current is assumed as shown in Fig.2. The longitudinal electric field is plotted together(red line). With these parameters, the calculation result from Eq.3 is  $E_s = 6.78$  V/m. Thus, within the rise region and fall region of this trapezoidal profile, the electric field is 6.78 V/m. In the FFT method, time length of 12  $\mu$ s is chosen and divided into 500 bins, and filled with 10k macro-particles that produce the same trapezoidal profile. Fig.2 shows that the peak electric field is almost the same as that calculated by Eq.3. In order to obtain more accurate electric fields in these regions, a larger bin number and accordingly, a larger macro-particle number seem to be required. However, that would increase the computation time; therefore a compromise must be made between the computation time and resolution.

**Initial distribution** As mentioned, the pulse length of the beam from the ECRIS before being chopped is about 5 ms. For He<sup>1+</sup> at 200 keV, the revolution time just after injection is about 12  $\mu$ s(given that KEK-DA’s main ring has

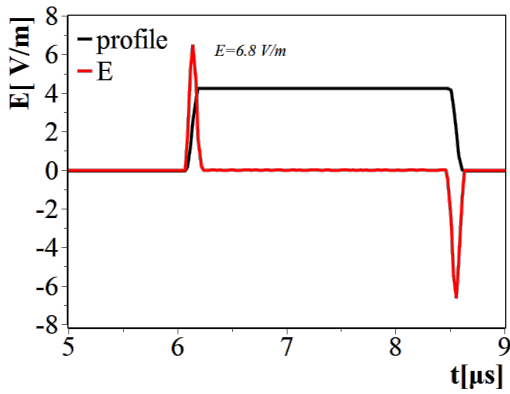


Figure 2: Justification of the FFT method.

a circumference of 37.7 m). Usually a 3 μs beam bunch is used in beam commissioning. The initial distribution includes a pulse profile of the bunch and a momentum distribution associated with this pulse profile. It has been realized that momentum modulation is induced at the head and tail of the beam bunch when the beam is chopped by the Einzel lens chopper[9]. A momentum distribution similar to the simulation results in Ref.[9] is assumed here.

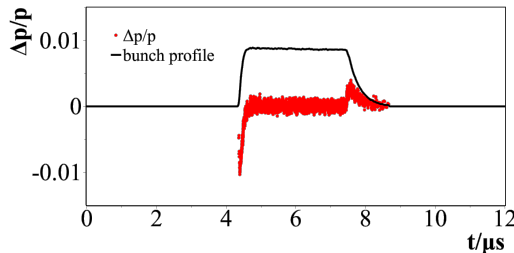


Figure 3: Initial distribution for simulation.

The black line is assumed pulse profile, which corresponds to the bunch signal captured by the wall current bunch monitor in experiments. Note that the l.h.s is bunch head and r.h.s is bunch tail. The red scattering dots are macro-particles in the phase space, where the bunch head part has a negative momentum deviation with a maximum of -1% while the tail part 0.5%. In addition, an “intrinsic” momentum deviation of  $\sigma = 0.05\%$  and  $2\sigma$  cut-off is assumed.

The distribution is assumed just after the post-acceleration column after which the bunch has a kinetic energy of 200 keV. Though at this momentum, there’s no good method to confirm the momentum distribution directly by measurement, the beam current and profile can be measured at the test stand with a Faraday cup which is 2.5 meters down from the post-acceleration column.

Fig.4 is the measurement result by Faraday cup.

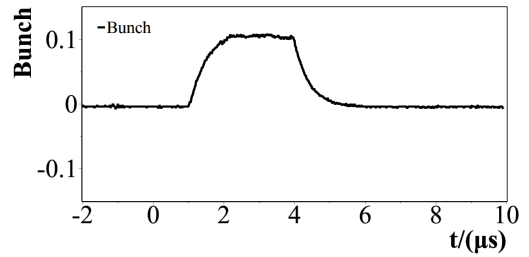


Figure 4: Bunch signal by Faraday cup.

## COMPARISON BETWEEN EXPERIMENTAL RESULTS AND SIMULATION

### Bunch Profile Evolution

Fig.5 shows turn-by-turn plots by plotting all the bunch signals one after another for a 3 μs He<sup>1+</sup> under the constant magnetic field without confinement or acceleration.

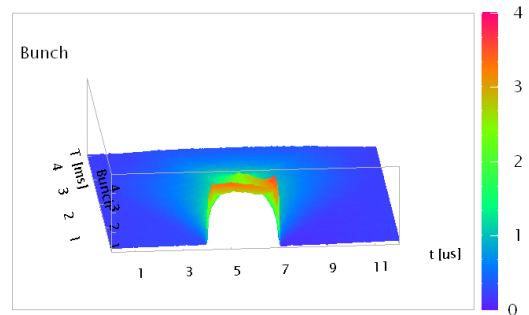


Figure 5: Mountain view of the observed bunch profile.

The horizontal axis,  $t[\mu s]$  is time position within one revolution(single bunch signal). The second axis,  $T[ms]$ , denotes the time from the injection for each bunch signal, corresponding to different turn number. The third axis is the beam current intensity. Fig.5 shows that the bunch structure gradually decays to fill the ring within 4 ms as the intensity drops.

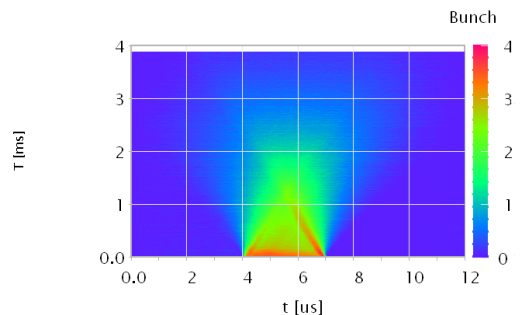


Figure 6: Projection of Mountain view.

Fig.6 shows the projected view of Fig.5 to the plane of the first and second axis(hereafter called time-turn plane).

The projection view is much easier to show the result thus will be frequently used later.

As seen in both Fig.5 and Fig.6, there's a peak at bunch head (l.h.s) and another one at the bunch tail(r.h.s). Moreover, the peak at the bunch tail survives for a longer time period and sharper than that at the bunch head. Besides, in fact for this result, those signals from the bunch monitor at the beginning are saturated. So peaks on bunch head and tail are much higher. However, the Faraday Cup measurement shows no such peaks.

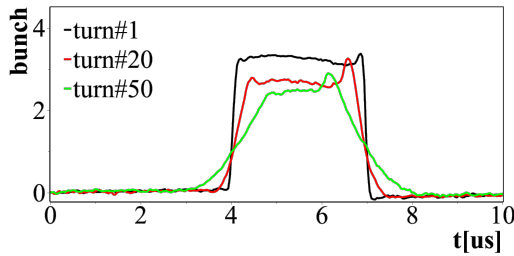


Figure 7: turn#1, #20,#50 of the experiment for  $3\mu\text{s He}^{1+}$  bunch,  $I = 50\mu\text{A}$ .

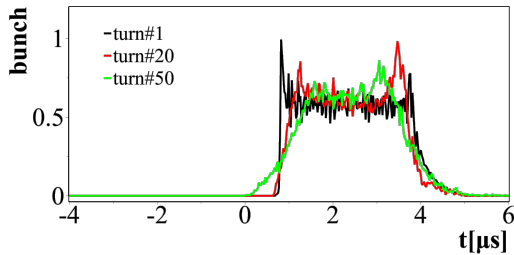


Figure 8: simulation with longitudinal space charge forces.

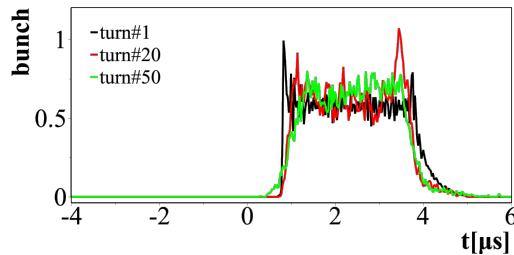


Figure 9: simulation without longitudinal space charge forces.

Fig.7 shows pulse signals of turn#1, #20 and #50 for the same experiment in Fig.5 and Fig.6. The beam current for this experiment was about  $50\mu\text{A}$ . This figure shows how the bunch profile evolves. Fig.8 shows the simulation result assuming a beam current of  $I = 50\mu\text{A}$ , taking into account of longitudinal space charge forces. Except for the first turn (which is supposed to be like the first signal on oscilloscope in experiment), the typical temporal evolution of the bunch profile, where the bunch tends to diffuse in the time axis and two peaks emerge at both ends of the bunch, is well

reproduced. The difference, if noticed, should come from the difference between initial distribution assumed in Fig.3 and that of the real beam bunch. For comparison, the simulation result without longitudinal space charge forces is shown in Fig.9. Compared with Fig.9, Fig.8 shows clearer peak formation and that the beam diffuses faster. The results on time-turn plane suggest the same observations as shown in Fig.10 and Fig.11.

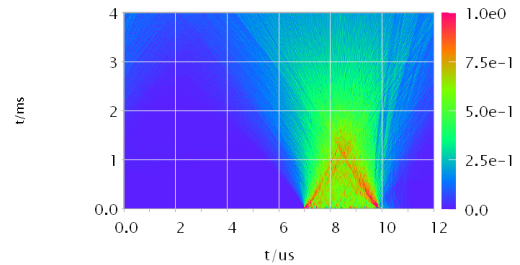


Figure 10: simulation with longitudinal space charge force.

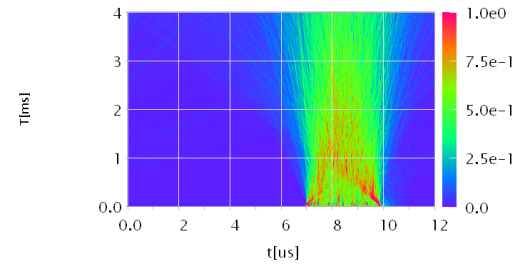


Figure 11: simulation without longitudinal space charge force.

The simulation without longitudinal space charge forces fails to reproduce the experimental result. On the contrary, the longitudinal space charge forces not only succeed in reconstructing the overall profile but also give the same cross point where two peaks finally meet, as seen from Fig.6 and Fig.10. The peak on the bunch head meet the bunch tail's at around  $1\text{ ms}$  after injection, or  $70 \sim 80$  turns after injection.

All these results suggest that longitudinal space charge forces are essential to understand how the bunch profile evolves like this.

When considering about longitudinal space charge forces, as indicated by Eq.3, higher beam current will have higher electric field. Comparisons between the experimental and simulation results including the longitudinal space charge forces for two beam currents of  $22\mu\text{A}$  and  $49\mu\text{A}$  are given in Figs.12, 13, 14, and 15.

In Fig.12 to Fig.15, they're different runs from that shown in Fig.10. However, the result of  $49\mu\text{A}$  is close to that of  $50\mu\text{A}$ . In present simulation, same intrinsic momentum deviation is assumed through all cases. In addition, the initial momentum deviation may depend on the beam current. These may explain why there exists slight difference between the experimental result and simulation

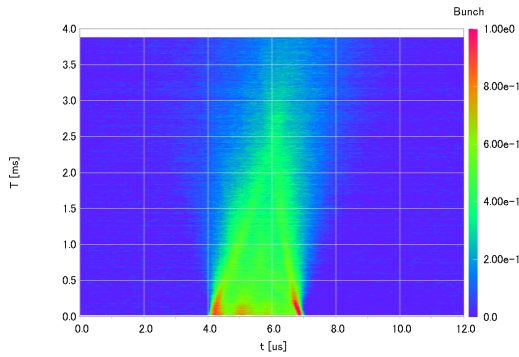


Figure 12: He<sup>1+</sup>, 22μA, experiment.

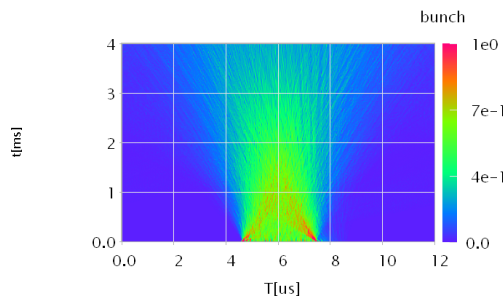


Figure 13: He<sup>1+</sup>, 22μA, simulation.

for 22 μA. But as in all, both of the experimental results and simulation strongly support the fact that for higher beam current the bunch head peak and tail peak will meet earlier.

*The Role of Longitudinal Space Charge Force*

It is understandable that the peak formation results partly from the initial momentum distribution as shown in Fig.3. Particles with negative momentum deviation in the bunch head move towards the positive direction in time, that is, the bunch tail. Because of the negative slippage factor,  $\eta$  (as  $\gamma < \gamma_t$ ). Particles with positive momentum deviation in the tail region will move towards the bunch head. Eventually, they will meet somewhere in the middle to form the cross point seen on Fig.6 and Fig.10. However, the simulation re-

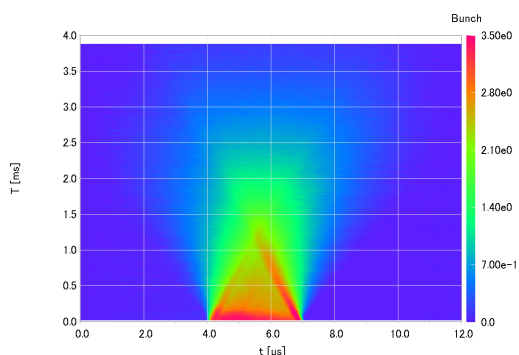


Figure 14: He<sup>1+</sup>, 49μA, experiment.

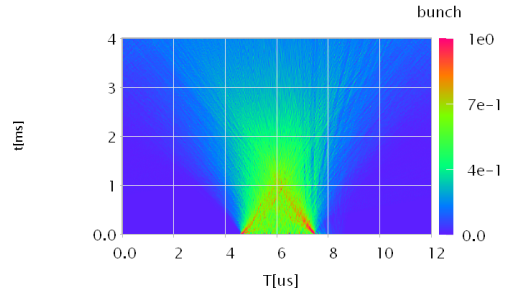


Figure 15: He<sup>1+</sup>, 49μA, simulation.

sult in Fig.11 shows that, without longitudinal space charge forces, these peaks dissipate quickly thus no apparent cross point.

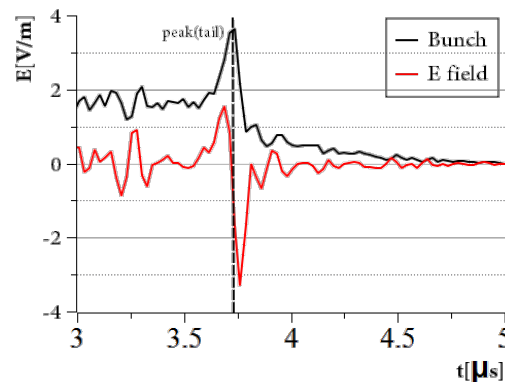


Figure 16: He<sup>1+</sup>, 49μA, tail part and associated electric field in simulation.

In order to explain the role of longitudinal space charge forces, Fig.16 shows the tail part of the bunch with electric field. At beginning, the peak comes into exist due to positive momentum deviation as just discussed. The dash line in Fig.16 marks the position of the peak. On the right side of the peak, the electric field is negative so that particles in this region will be kick down by the longitudinal charge forces in the phase space. If this field is large enough then these particles will have a negative momentum deviation and move to the right, making the bunch become longer, or bunch is spreading in the longitudinal direction. Because at the beginning the momentum deviation in this region is positive, so space charge forces make these particles slow down as they move to the left side. After that, once particles fall into negative momentum deviation region, they will move to the right and make the bunch spread. Without longitudinal space charge forces, bunch will only spread according to the momentum spread, which is much slower as seen in Fig.9. If only the electric field on the right side of the peak the beam is considered, the bunch will spread as discussed and the peak will disappear quickly. However, as noted in Fig.16, the electric field due to longitudinal space charge forces is positive, that is, this field will kick particles in that region upward. Because these particles have a

larger momentum deviation than the intrinsic momentum deviation, new peak will emerge just as the peak formation happens at the very beginning. The total effect of the electric field on both sides of the peak is that the peak lasts for a longer time. Because the electric field on the left side of the peak is smaller than the right, the peak will become smaller and appear not so obvious, as seen in Fig.12 and Fig.13. For higher beam current, the peak will last for such a longer time that two peaks on the bunch head and tail will merge when they meet each other, forming a cross point, as seen in Fig.14 and Fig.15. How fast a particle will move in phase space depends on its momentum deviation. As a result, in case of higher beam current, due to the role of the electric field on the left side of the peak shown in Fig.16, affected particles will have a larger momentum deviation and move faster towards the beam center. That's why bunch with higher beam current has an earlier cross point when comparing Fig.12 and Fig.14.

## CONCLUSION AND FUTURE WORK

As in short, the Einzel lens chopper induces a momentum modulation on the bunch head and tail while chopping the beam. Then longitudinal space charge forces affect a great deal of the bunch profile evolution and peak formation. Because KEK-DA is an induction synchrotron capable of accelerating ion beam from a very low energy to relatively high energy, the space charge force is one of the most important topics in the beam physics related to it. More studies and results where space charge force plays an essential role could be anticipated.

The beam commissioning will go on and some application studies by using KEK-DA would follow. As for the simulation, which is now short of motion of transverse direction, will include it to be a more useful tool for beam commissioning and analysis.

## ACKNOWLEDGEMENT

This work is supported by a Grant-In-Aid for Scientific Research (A) (KAKENHI NO.23240082).

## REFERENCES

- [1] K.Takayama, and J.Kishiro, Induction Synchrotron, Nucl. Inst. Meth. Phys. Res. A 451, 304 (2000).
- [2] Takayama, K., Arakida, Y., Dixit, T., Iwashita, T., Kono, T., Nakamura, E., Otsuka, K., et al. (2007). Experimental Demonstration of the Induction Synchrotron. Physical Review Letters, 98(5), 8-11.
- [3] T. Iwashita et al., KEK Digital Accelerator, Phys. Rev. ST-AB 14, 071301 (2011). And K.Takayama et al., in this conference.
- [4] K.Takayama and R.J.Briggs (Eds), Induction Accelerators, (Springer, 2010).
- [5] T. Adachi, T. Arai, K. W. Leo, K. Takayama, and A. Tokuchi, A Solid-State Marx Generator Driven Einzel Lens Chopper, Rev. Sci. Instrum. 82, 083305 (2011).
- [6] Leo Kwee Wah, K.Takayama, T.Arai, et al., Permanent Magnet ECRIS for the KEK Digital Accelerator, Proceedings of 19th International workshop on ECR Ion Sources, August 23rd -26th, 2010 Grenoble, France, Pg. 150 (2010).
- [7] S.Harada, Ms. Thesis (Tokyo City University) (2011).
- [8] MacLachlan, J. A., Longitudinal Phase Space Tracking With Space Charge and Wall Coupling Impedance, FermiLab Note, FN-446, (1987).
- [9] K.W.Leo, Doctor Thesis(The Graduate University For Advanced Studies)(2012).